JOURNAL OF MATERIALS SCIENCE 31 (1996) 3109–3114

Determination of the hardness and elastic modulus from continuous Vickers indentation testing

J. GUBICZA, A. JUHÁSZ, P. TASNÁDI, P. ARATÓ*, G. VÖRÖS
Department of General Physics, Eötvös University, Budapest, H-1088 Budapest, Múzeum krt. 6–8 Hungary
** Research Institute for Technical Physics, P.O.B. 76, H-1325, Budapest, Hungary*

Continuous Vickers (H_V) indentation tests were performed on different materials (ion crystals, metals, ceramics, silica glass and plastic). Load–indentation depth curves were taken during the loading as well as during the unloading period by a computer controlled hydraulic mechanical testing machine (MTS 810). The indentation work measured both the loading and the unloading periods, and these were used for the evaluation of parameters characterizing the materials. It was found empirically that there were linear connections between the maximum load to the power 3/2 and the indentation work. These connections were used to relate the conventional hardness number, H_V, and Young's modulus, E, with the work performed during loading and unloading. This work can be determined with great accuracy from the measurements. The values of the Young's modulus and the Vickers hardness determined this way agree well with those obtained by conventional methods. On the basis of continuous indentation tests, materials can be easily classified into the isomechanical groups introduced by Ashby. For this classification the H_V/E ratio is generally used. As a substitute for H_V/E another parameter is recommended which can be determined easily from a single measurement.

1. Introduction

Various types of continuous indentation tests have come into general use for the determination of mechanical properties of materials. The indentation method is preferred because relatively small amounts of testing material are needed and there are no strict requirements for the shape of the samples, moreover the measurements can be performed without the destruction of the samples. For these investigations a wide variety of testing devices were developed with indenters of various forms working in a scale from the nanoidentation to macrohardness region. The common feature of these tests is that the applied load is registered as a function of indentation depth during both the loading and unloading period [1–6].

A schematic load–penetration depth curve is shown in Fig. 1. The curves taken during loading and unloading can be described by polynoms [1, 3–6] or power law functions [2]. The parameters of these functions depend intricately on both the elastic and the plastic properties of the samples investigated because materials are generally deformed both elastically and plastically by a sharp indentor. Therefore, to find out the conventional elastic and plastic parameters of a material from the continuous indentation tests is not a simple problem. However, there are various theoretically more or less well supported methods for the evaluation of the load–penetration depth functions obtained experimentally.

Fröhlich *et al.* [1] studying the connection between the hardness number and the parameters of the indentation curve described the loading period by a quadratic polynom. He proposed that the coefficient of the quadratic term can be regarded as a new hardness number characterizing the resistance of the bulk material against elastic–plastic deformation. The main advantage of the use of this parameter is that it is independent of the magnitude of the load and consequently from the diagonal of the Vickers pattern. As is well known, the conventional hardness number is by definition the maximum load divided by the contact area of the indenter and the sample measured at maximum load [7–10]. Direct calculation of the conventional hardness number from a continuous indentation test is difficult because generally there is no simple way for the determination of the contact area. Oliver and Pharr [2] elaborated on an iterative procedure for the determination of the projected area of the contact surface. It needed the maximum penetration depth and the slope of the unloading curve at its starting point as initial parameters. The uncertainty of both parameters is relatively high. For the first quantity it is the consequence of the uncertainty of the measurement of the load, for the second one it is due to the fact that the calculated value of the slope of the unloading curve depends strongly on the form of the function fitted to the unloading curve.

0022–2461

Methods available in the literature for the calculation of Young's modulus from indentation tests are based in most cases on the theoretical solution of the Boussinesq problem given by Sneddon [11] who determined the indentation depth within an elastic half space for various indenters. Pharr *et al.* [12], using Sneddon's results, have calculated the reduced Young's modulus, E_r, [$(E_r = E/1 - v^2)$ where E is the Young's modulus and v is the Poisson's ratio] for a broad variety of materials. Their input data were in this case also the slope of the initial part of the unloading curve and the contact area of the indenter and the sample at the maximum load.

Sakai [4] applied a Maxwell type elastic–plastic model for the description of the indentation process. He defined a so-called "true hardness" for the characterization of the plastic properties of the materials and determined it from the energy dissipated during a loading–unloading period. Sakai also determined the reduced Young's modulus from the unloading curve; however, he did not take into account that this curve depended not only on the elastic but also on the plastic properties of the materials.

In the present paper a detailed analysis of the continuous indentation curves is given and a new method based on energetic argumentation is proposed for the determination of the hardness number and the Young's modulus.

2. Experimental procedure

The mechanical properties of the materials were investigated by a special kind of continuous Vickers hardness test. The surface of the samples was mechanically polished before measurement. During the test a Vickers pyramid was pressed into the surface of the sample by a computer controlled hydraulic mechanical testing machine (MTS 810). The measurements were carried out in the macrohardness region ($P_{max} \approx 100$ N). During the loading period the Vickers pyramid penetrated into the surface of the sample at constant velocity and the same velocity was applied in the unloading period when the pyramid moved backwards. In the course of the test the load was registered as a function of the penetration depth. Measurements were performed on various materials: metals (99.99% pure Al and Cu), soda lime silica glass, alkali halogenide crystals, polypropylene, Si_3N_4 ceramics of a composition 90 wt % Si_3N_4–4 wt % Al_2O_3–6 wt % Y_2O_3 sintered to different densities and a series of alumina–hydroxyapatite ceramic composites (Al_2O_3–HAP) with alumina contents up to 60 vol %, and a tetragonal zirconia polycrystal ceramic sample containing 10 mol % CeO_2 (Ce–TZP ceramic).

3. Results and discussion

3.1. Features of the indentation curves

In the loading period the load–penetration depth function can be described by a quadratic polynom (Fig. 1)

$$P = c_2 h + c_3 h^2 \qquad (1)$$

For the unloading period the load also satisfies a quadratic equation

$$P = c_2^*(h - h_0) + c_3^*(h - h_0)^2 \qquad (2)$$

where P is the load; h is the penetration depth; h_0 is the residual indentation depth after removing the punch; and c_2, c_3, c_2^*, c_3^* are fitting parameters. The total indentation work is the integral of the load with respect to the indentation depth and it equals to the area under the load–penetration depth curve corresponding to the loading period. During unloading a portion of this work can be regained, it is equal to the area under the load–indentation depth curve for this latter period.

The difference between these two calculations for work gives the energy dissipated during the loading–unloading period (Fig. 1). The work performed during loading, W_t, and unloading, W_e, can be calculated by integration of Equations 1 and 2, respectively

$$W_t = \frac{c_2}{2} h_m^2 + \frac{c_3}{3} h_m^3 \qquad (3)$$

$$W_e = \frac{c_2^*}{2}(h_m - h_0)^2 + \frac{c_3^*}{3}(h_m - h_0)^3 \qquad (4)$$

where h_m is the maximum indentation depth. The difference between the two quantities equals the work dissipated, i.e.

$$W_d = W_t - W_e \qquad (5)$$

If the load–penetration depth functions were quadratic ($c_2 = c_2^* = 0$), all three calculations for work should be proportional to $P_m^{3/2}$. In spite of the fact that the experimental results show that these functions are not quadratic for the materials investigated, the linear relationship between the works and $P_m^{3/2}$ is still a good approximation. This fact is illustrated in Fig. 2, where the total indentation work is shown as a function of $P_m^{3/2}$ for copper. It can be proved that even if the contribution of the linear term in Equation 1 reaches 40 per cent of the maximum load, the $W_t/P_m^{3/2}$ ratio

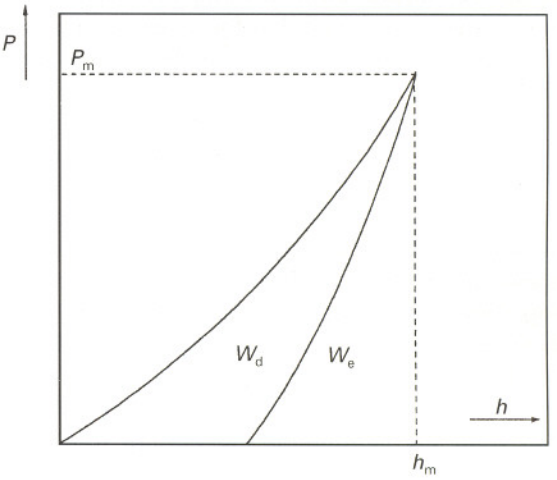

Figure 1 Schematic picture of an indentation cycle: P, load; P_m, maximum load; W_d, work dissipated; W_e, work performed during unloading; h, indentation depth.

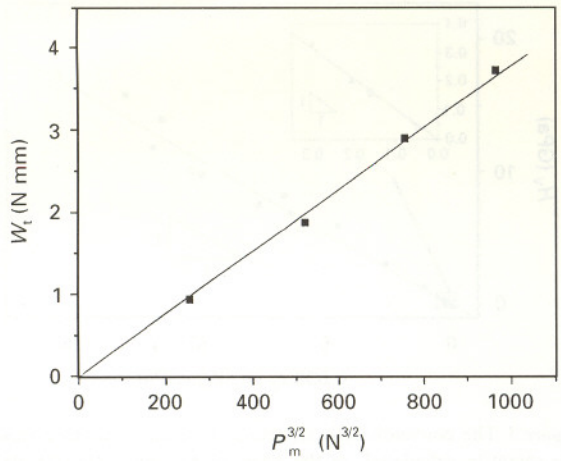

Figure 2 The total work, W_t, performed on copper depends linearly on $P_m^{3/2}$ (where P_m is the maximum load).

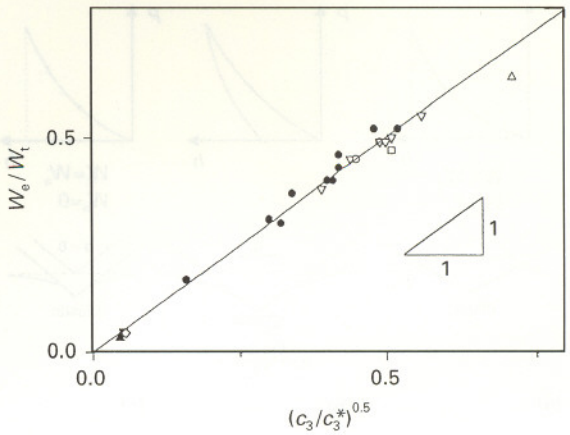

Figure 3 The ratio of the elastic and total work versus the parameters of the indentation curves: (△) glass, (▲) Al, (▼) Cu, (◇) NaCl, (●) Si_3N_4, (□) plastic, (▽) Al_2O_3–HAP, (○) Ce–TZP.

differs only by 7 per cent from the value calculated from the quadratic function.

The quadratic term of the load–penetration depth function as a fraction of maximum load can be expressed by the following

$$k \times P_m = c_3 \times h_m^2 \quad (6)$$

According to the author's measurements for the different materials investigated, k varies between 0.6 and 0.9. Similarly the cubic term in the total work function can be expressed as a fraction of the total work

$$k' \times W_t = \frac{c_3}{3} \times h_m^3 \quad (7)$$

With the help of these functions the following relationship can be derived between W_t and $P_m^{3/2}$

$$W_t = \frac{k}{k'} k^{1/2} \frac{1}{3(c_3)^{1/2}} P_m^{3/2} \quad (8)$$

Since c_3 is a constant depending only on the material investigated, this relationship would be linear for a given material if $(k/k')k^{1/2}$ were constant. Of course this condition is generally not strictly satisfied. Nevertheless it can be shown (see Appendix) that in the range $k \geqslant 0.6$ this quantity varies only slightly, therefore the $W_t(P_m^{3/2})$ function is nearly linear. Consequently, using the formulae derived in the Appendix, the experimental results can be satisfactorily described well by the following relationships

$$W_t = m \times P_m^{3/2} \quad (9)$$

$$W_e = m^* \times P_m^{3/2} \quad (10)$$

$$W_d = \bar{m} \times P_m^{3/2} \quad (11)$$

where

$$m = \frac{1}{3(c_3)^{1/2}} \quad (12)$$

$$m^* = \frac{1}{3(c_3)^{1/2}} \quad (13)$$

$$\bar{m} = m - m^* = \frac{1}{3}\left[\frac{1}{(c_3)^{1/2}} - \frac{1}{(c_3^*)^{1/2}}\right] \quad (14)$$

According to Equations 9–14 it is obvious that the works and the parameters of the load–indentation depth functions should also satisfy the following relationship

$$\frac{W_e}{W_t} = (c_3/c_3^*)^{1/2} \quad (15)$$

Fig. 3 shows that the experimental data fit well to Equation 15 for a broad variety of materials.

3.2. The connection between the conventional hardness number and the parameters of the indentation curves

The parameter c_3 which can be easily determined from the loading curve is generally used for the characterization of the hardness of materials, however, it is not equal to the conventional hardness number [1, 4].

In the case of an ideally plastic material the load–indentation depth function is quadratic: $P = c_3 h^2$ [4, 13]. Since there is no elastic relaxation, the $d = 7\ h_m$ equation between the diagonal of the Vickers pattern, d, and the indentation depth, h_m, which is the consequence of the geometry of the Vickers pyramid is exactly satisfied (Fig. 4a). Therefore the Vickers hardness of the ideally plastic materials obeys the following equation

$$H_V = 1.8544 \times \frac{P_m}{d^2} = 1.8544 \times \frac{P_m}{49 \times h_m^2} = \alpha_1 \times c_3 \quad (16)$$

where $\alpha_1 = 0.038$.

If the material is not ideally plastic then with increasing contribution of the elastic deformation to the total one, elastic deflection of the material under the indenter increases (Fig. 4b). Consequently $7h_m$ becomes step by step larger than d, and as a result of this $\alpha_1 \times c_3$ will be less than H_V.

The authors have sought a relationship between H_V and $\alpha_1 \times c_3$ in the form of

$$H_V = \beta \alpha_1 c_3 \quad (17)$$

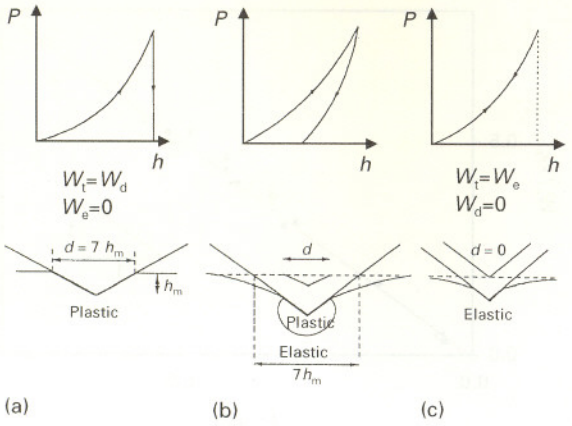

Figure 4 Schematic picture showing the behaviour of various materials during Vickers indentation: (a) ideally plastic, (b) elasto–plastic, and (c) ideally elastic.

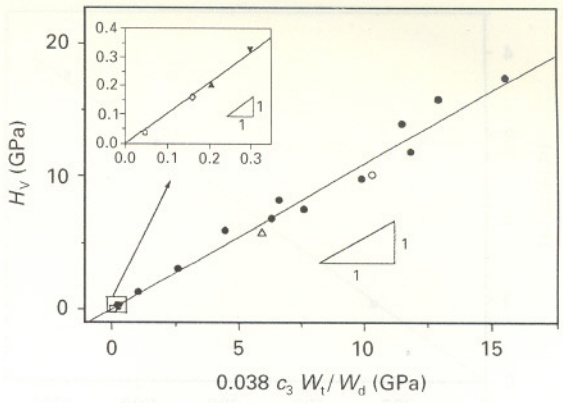

Figure 5 The conventionally determined hardness number versus the quantity calculated on the basis of Equation 18: (△) glass, (▲) Al, (▼) Cu, (◇) NaCl, (●) Si_3N_4, (□) plastic, (○) Ce–TZP.

It is obvious that β must be one for an ideally plastic material and with increasing elasticity it must increase; and in the limiting case of an ideally elastic material it becomes infinite, because in this case there is no residual deformation after unloading (Fig. 4). The $\beta = W_t/W_d$ ratio satisfies the conditions imposed on the limiting cases and according to the present measurements the experimental results fit well for a broad variety of materials to the equation (Fig. 5)

$$H_V = \alpha_1 \times c_3 \times \frac{W_t}{W_d} \tag{18}$$

3.3. The connection between the parameters of the indentation curves and the Young's modulus

A similar relationship has been found between the parameters of the load–penetration depth curves and the Young's modulus. According to the theoretical investigation of Sneddon [11] the load–indentation depth function for an ideally elastic material (Fig. 4c) can be described in both the loading and the unloading period by the same equation

$$P = c_3 h^2 = c_3^* h^2 \tag{19}$$

where

$$c_3 = c_3^* = \frac{E}{2(1-\nu^2)} \times \frac{\alpha_0}{\gamma^2} \times \tan\Psi \tag{20}$$

where E is the Young's modulus, ν is the Poisson's ratio, α_0 is a constant depending on the geometry of the indenter ($\alpha_0 = 2$ for Vickers indenter), $\gamma = (\pi/2)$, ψ is the semi-angle of the indenter (74.05° for a Vickers indenter) [11, 13, 14]. From this equation the Young's modulus of ideally elastic materials can be given in the form

$$E = \alpha_2 c_3^* \tag{21}$$

with

$$\alpha_2 = \frac{2(1-\nu^2)\gamma^2}{\tan\Psi\,\alpha_0} \tag{22}$$

Substituting into these equations the parameters characterizing the geometry of the Vickers pyramid and taking ν as 1/3 one gets $\alpha_2 = 0.63$. Empirical evidence shows that Equation 21 is not valid for materials where the deformation is not ideally elastic. In these cases $\alpha_2 c_3^*$ becomes higher than E. This can be explained in the following way. In the course of the plastic deformation a plastic zone is developing under the indenter (Fig. 4b) and due to this the elastic stresses and deformations are lower at the same E and P_m than they would be in an ideally elastic material. Consequently, elastic relaxation is also smaller than in the ideally elastic case. Assuming a relationship between E and $\alpha_2 c_3^*$ in the form

$$E = \beta' \alpha_2 c_3^* \tag{23}$$

the β′ factor must be one for ideally elastic materials and it must decrease with increase of the plastic fraction of the deformation. Of course, in the ideally plastic limit E must tend to infinity. According to the experimental results the ratio of the elastic and total work performed in the course of a loading–unloading cycle can be used as β′, i.e. Equation 23 can be written in the following form

$$E = \alpha_2 c_3^* \frac{W_e}{W_t} \tag{24}$$

In the elastic limit this formula immediately yields Equation 21, predicted theoretically. In the ideally plastic limit the validity of $E \to \infty$ is not so obvious, because although $c_3^* \to \infty$, (W_e/W_t), as mentioned already, tends to zero. However, rearranging Equation 24 with the help of Equation 15 one can get

$$E = \alpha_2 c_3 \frac{W_t}{W_e} \tag{25}$$

This formula implies $E \to \infty$ for the ideally plastic limiting case, since c_3 is a finite number and (W_t/W_e) tends to infinity. Fig. 6 shows that Youngs' moduli measured by the four-point bending test agree relatively well with those calculated on the basis of Equation 25. The deviation is especially significant for the

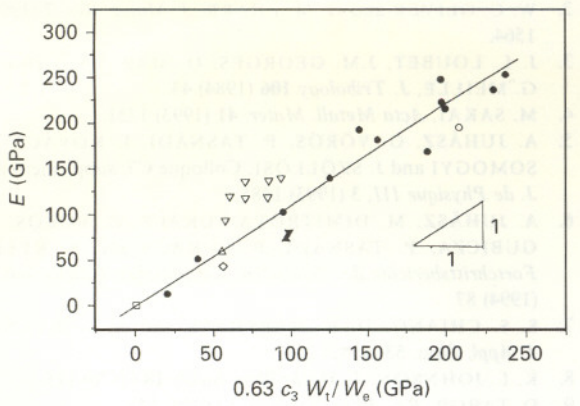

Figure 6 Relationship between Young's modulus determined by four-point bending test and that calculated on the basis of Equation 25: (△) glass, (▲) Al, (▼) Cu, (◇) NaCl, (●) Si_3N_4, (□) plastic, (▽) Al_2O_3–HAP, (○) Ce–TZP.

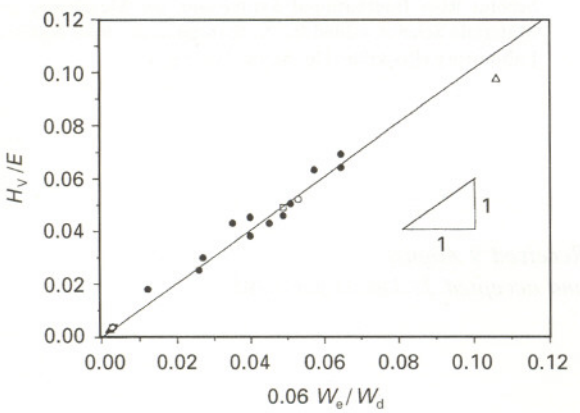

Figure 7 The H_V/E ratio as a function of 0.06 (W_e/W_d): (△) glass, (▲) Al, (▼) Cu, (◇) NaCl, (●) Si_3N_4, (□) plastic, (○) Ce–TZP.

Al_2O_3–HAP series which may be caused by taking $\nu = 1/3$ for the calculation of α_2.

3.4. The isomechanical groups

Ashby and Brown classified materials into isomechanical groups on the basis of the H_V/E ratio [15]. Dividing Equation 18 by Equation 25 one gets

$$\frac{H_V}{E} = \alpha_3 \frac{W_e}{W_d} \tag{26}$$

where $\alpha_3 = 0.06$. Fig. 7 shows that the ratio of the hardness and the elastic modulus is proportional to the ratio of the elastic and the dissipated work. The experimental results prove that using the work performed in an indentation cycle, the Ashby type classification can be easily done because the indentation work can be determined with great accuracy from the continuous indentation measurements. It is worth mentioning that the c_3 parameter in Equations 18 and 25 for the expressions of H_V and E, respectively, can be calculated with higher accuracy from the m, m^* and $\bar{m}$ parameters of Equations 12–14 than directly from the load–indentation depth functions. The reason for this is probably the uncertainty in the determination of the starting point of the loading curve. Therefore using Equations 9–14 one has derived the following formulae for the determination of H_V, E and the H_V/E ratio

$$H_V = \frac{\alpha_1}{9} \frac{1}{m\bar{m}} \tag{27}$$

$$E = \frac{\alpha_2}{9} \frac{1}{mm^*} \tag{28}$$

$$\frac{H_V}{E} = \alpha_3 \frac{m^*}{\bar{m}} \tag{29}$$

4. Conclusions

A linear relationship was empirically found between the indentation work determined in the loading and unloading period and $P_m^{3/2}$, where P_m was the maximum load of the indentation cycle. Relationships between the conventionally measured Vickers hardness, Young's modulus and the parameters of the indentation curves were established. The equations obtained empirically satisfy the conditions imposed on the ideally elastic and plastic limiting cases.

It also has been proved that the ratio of the elastic and the dissipated work performed during an indentation cycle can be used instead of the H_V/E ratio, on the basis of which the materials can be classified into isomechanical groups.

Appendix

To investigate the linearity of the $W_t(P_m^{3/2})$ function the quantity $(k/k')k^{1/2}$ can be expressed as a function of k. Take the ratio of the two terms in P_m and W_t, respectively

$$\frac{k}{1-k} = \frac{c_3 \times h_m^2}{c_2 h_m} = \frac{c_3 h_m}{c_2} \tag{A1}$$

$$\frac{k'}{1-k'} = \frac{c_3 h_m^3/3}{c_2 h_m^2/2} = \frac{2 \times c_3 h_m}{3 \times c_2} \tag{A2}$$

From these equations one gets

$$k' = \frac{2k}{3-k} \tag{A3}$$

Using Equation A3 one can obtain

$$\frac{k}{k'} k^{1/2} = \frac{(3-k)k^{1/2}}{2} = f(k) \tag{A4}$$

Fig. 8 shows $f(k)$ as a function of k. It can be seen that if $k \geqslant 0.6$ then $f(k) \geqslant 0.93$.

It means that since for these present measurements $k \geqslant 0.6$, $f(k)$ is approximately constant which equals to one and there is a linear connection between W_t and $P_m^{3/2}$. On the basis of Equations 2 and 4 a similar relationship can be derived for W_e, i.e. it can be shown that $W_e(P_m^{3/2})$ is also a linear function.

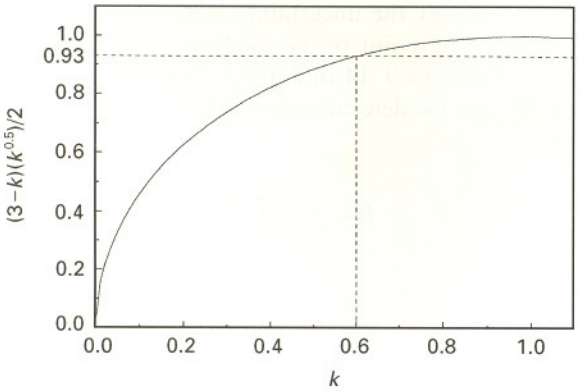

Figure 8 The $f(k)$ function.

Acknowledgements

The authors are grateful to M. Dimitrova-Lukács for providing the Al_2O_3-*HAP* and Ce-TZP ceramic samples and Professor J. Lendvai for very helpful discussions and comments. This work was supported by the Hungarian National Scientific Fund in contract number T-017637, T-017639 and T-017474.

References

1. F. FRÖHLICH, P. GRAU and W. GRELLMANN, *Phys. Status Solidi* (*a*) **42** (1977) 79.
2. W. C. OLIVER and G. M. PHARR, *J. Mater. Res.* **7** (1992) 1564.
3. J. L. LOUBET, J.M. GEORGES, O. MARCHESINI and G. MEILLE, *J. Tribology* **106** (1984) 43.
4. M. SAKAI, *Acta Metall. Mater.* **41** (1993) 1751.
5. A. JUHÁSZ, G. VÖRÖS, P. TASNÁDI, I. KOVÁCS, I. SOMOGYI and J. SZÖLLÖSI, Colloque C7, supplément au *J. de Physique III*, **3** (1993) 1485.
6. A. JUHÁSZ, M. DIMITROVA-LUKÁCS, G. VÖRÖS, J. GUBICZA, P. TASNÁDI, P. LUKÁCS and A. KELE, *Fortchrittsberichte der Deutschen Keramischen Gesellschaft* **9** (1994) 87.
7. S. S. CHIANG, D. B. MARSHALL and A. G. EVANS, *J. Appl. Phys.* **53** (1982) 298.
8. K. L. JOHNSON, *J. Mech. Phys. Solids* **18** (1970) 115.
9. D. TABOR, *Rev. Phys. Technol.* **1** (1970) 145.
10. *Idem*, "Hardness of Metals" (Clarendon Press, Oxford, 1951).
11. I. N. SNEDDON, *Int. J. Engng Sci.* **3** (1965) 47.
12. G. M. PHARR, W. C. OLIVER and F. R. BROTZEN, *J. Mater. Res.* **7** (1992) 613.
13. B. R. LAWN and V. R. HOWES, *J. Mater. Sci.* **16** (1981) 2745.
14. A. E. H. LOVE, *Q. F. Math.* **10** (1939) 161.
15. M. F. ASHBY and A. M. BROWN, in Proceedings of the Second Riso International Symposium on Metallurgy and Materials Science, edited by N. Hansen *et al.*, Riso National Laboratory (Roskilde, Denmark, 1981) p. 1.

Received 9 August
and accepted 21 December 1995